

# Human Transcriptional Coactivator with PDZ-Binding Motif (TAZ) Is Downregulated During Decidualization<sup>1</sup>

Zuzana Strakova,<sup>2</sup> Jennifer Reed, and Ivanna Ihnatovych

Department of Obstetrics and Gynecology, University of Illinois at Chicago, Chicago, Illinois

## ABSTRACT

Transcriptional coactivator with PDZ-binding motif (TAZ) is known to bind to a variety of transcription factors to control cell differentiation and organ development. However, its role in uterine physiology has not yet been described. To study its regulation during the unique process of differentiation of fibroblasts into decidual cells (decidualization), we utilized the human uterine fibroblast (HuF) *in vitro* cell model. Immunocytochemistry data demonstrated that the majority of the TAZ protein is localized in the nucleus. Treatment of HuF cells with the embryonic stimulus cytokine interleukin 1 beta in the presence of steroid hormones (estradiol-17 beta and medroxyprogesterone acetate) for 13 days did not cause any apparent TAZ mRNA changes but resulted in a significant TAZ protein decline (approximately 62%) in total cell lysates. Analysis of cytosolic and nuclear extracts revealed that the decline of total TAZ was caused primarily by a drop of TAZ protein levels in the nucleus. TAZ was localized on the peroxisome proliferator-activated receptor response element site (located at position –1200 bp relative to the transcription start site) of the genomic region of decidualization marker insulin-like growth factor-binding protein 1 (IGFBP1) in HuF cells as detected by chromatin immunoprecipitation. TAZ is also present in human endometrium tissue as confirmed by immunohistochemistry. During the secretory phase of the menstrual cycle, specific TAZ staining particularly diminishes in the stroma, suggesting its participation during the decidualization process, as well as implantation. During early baboon pregnancy, TAZ protein expression remains minimal in the endometrium close to the implantation site. In summary, the presented evidence shows for the first time to date TAZ protein in the human uterine tract, its downregulation during *in vitro* decidualization, and its localization on the IGFBP1 promoter region, all of which indicate its presence in the uterine differentiation program during pregnancy.

*decidua, decidualization, human endometrium, IGFBP1 gene promoter, implantation, implantation site, pregnancy, TAZ, uterus*

## INTRODUCTION

The activation of specific programs of gene expression during cell differentiation and organ development depends on a combination of interactions among DNA-binding transcription

factors, transcriptional cofactors, and histone-modifying enzymes [1]. One such protein, transcriptional coactivator with PDZ-binding motif (TAZ, also called WWTR1), was originally identified as a 14-3-3-binding protein [2]. TAZ contains the WW domain and functions by binding to the PPXY motif present on transcription factors [2].

TAZ was reported to bind to a variety of transcription factors to control cell differentiation and organ development [3–8]. Its C-terminal contains a PDZ-binding motif that localizes TAZ in discrete nuclear foci [2]. TAZ represses transcription factor peroxisome proliferator-activated receptor gamma (PPARG)-dependent gene transcription during differentiation of mesenchymal stem cells into adipocytes [3]. In mice, PPARG is essential for the formation of a functional placenta [9]. Moreover, PPARG-induced gene networks were described as critical regulators of mouse implantation [10].

During implantation, trophoblast migration and invasive capacity have been shown to be modulated by numerous factors, including insulin-like growth factor-binding protein 1 (IGFBP1) [11, 12]. IGFBP1 is the major secretory product of the human decidualized endometrium [13] and is one of the markers of human decidualization. Decidualization is a major change that occurs in the endometrium after conception and involves the differentiation of stromal fibroblasts into decidual cells [14, 15]. Decidualization spreads from the implantation site to the whole uterine lining, and the decidua serves as a contact inhibition layer to trophoblast invasion for the duration of the pregnancy. Thus, decidualization is critical for the successful establishment and maintenance of pregnancy [14, 15]. Defects in decidualization were described in infertility patients and patients with endometriosis and were linked to preeclampsia [16–18]. The exact molecular mechanisms regulating this complex process of stromal cell transformation are still unknown. We previously demonstrated that an embryo-mimicking signal represented by proinflammatory cytokine interleukin 1 beta (IL1B) in the presence of steroid hormones (SHs) induces IGFBP1 expression in the human uterine fibroblast (HuF) *in vitro* decidualization model [19]. We have confirmed the relevance of IL1B for *in vivo* decidualization in the baboon model of simulated pregnancy [20]. The present study was aimed at investigating the role of TAZ in uterine physiology by examining its presence in the human uterine endometrium and its involvement in *in vitro* decidualization of human stromal fibroblasts.

## MATERIALS AND METHODS

### Materials

Recombinant human IL1B was obtained from R&D Systems, Inc. (Minneapolis, MN). The rabbit polyclonal antibody to TAZ used in Western blot detections was from Cell Signaling Technology, Inc. (Beverly, MA), and the TAZ antibody used in the chromatin immunoprecipitation (ChIP) assay was from Novus Biologicals (Littleton, CO). Purchased from Sigma (St. Louis, MO) were the following: the TAZ antibody (WWTR1) used for immunohistochemistry, monoclonal beta-actin antibody clone AC 15, and dibutyl cAMP

<sup>1</sup>Supported by National Institutes of Health American Recovery & Reinvestment Act of 2009 grant 2R01-HD44713 to Z.S.

<sup>2</sup>Correspondence: Zuzana Strakova, Department of Obstetrics and Gynecology, University of Illinois at Chicago, Chicago, IL 60612-7313. FAX: 312 996 4238; e-mail: zstrakov@uic.edu

Received: 5 October 2009.

First decision: 28 October 2009.

Accepted: 12 February 2010.

© 2010 by the Society for the Study of Reproduction, Inc.

eISSN: 1529-7268 <http://www.biolreprod.org>

ISSN: 0006-3363

(dbcAMP) and cAMP. Rhodamine-conjugated phalloidin was purchased from Molecular Probes (Eugene, OR). Prolong Antifade mounting medium containing 4',6'-diamidino-2-phenylindole (DAPI) and all cell culture supplies were obtained from Invitrogen (Grand Island, NY). Other reagents of cell culture grade were purchased from Fisher Scientific (Itasca, IL) or Sigma.

### Tissue Collection

Human placenta tissue and human endometrial tissues were obtained from the Human Female Reproductive Tissue bank in the Center for Women's Health and Reproduction at the University of Illinois at Chicago. All studies were approved by the Institutional Review Board of the University of Illinois. Baboon endometrial tissue was obtained from adult female baboons (*Papio anubis*) by endometriectomy or after hysterectomy. Uteri from pregnant baboons (Day 30 of pregnancy) were obtained after the pregnancy was confirmed as previously described [21]. After visualization of the site of conceptus attachment, the uterus tissue directly under the implantation site was used as the sample for immunohistological studies. The animal study was approved by the Animal Care Committee at the University of Illinois at Chicago.

### Cell Culture and Treatment with Decidualization Stimuli

HuF cells were isolated from the decidua parietalis, dissected from placental membranes after normal vaginal delivery at term as previously described [19]. These cells represent a proliferating population of nondifferentiated fibroblastic cells, which are maintained in the decidualized uterine endometrium and closely resemble endometrial stromal cells [22, 23]. HuF cells were confirmed as a suitable model for in vitro decidualization in studies by us and others [19, 22–27].

Cells were cultured in RPMI-1640 medium supplemented with 10% heat-inactivated and charcoal-stripped fetal bovine serum (SFBS), 0.1 mM sodium pyruvate, and 1% penicillin-streptomycin. At confluence, cells were trypsinized, propagated, and used for experiments in passage numbers three to five. Cell purity was assessed by immunocytochemistry using antibodies against cytokeratin (DAKO, Glostrup, Denmark) and vimentin (Zymed Laboratories, Inc., San Francisco, CA). The purity of fibroblast cells used in the studies was greater than 97%.

Decidualization studies were carried out in RPMI-1640 with 2% SFBS. Confluent HuF cells were subjected to vehicle control (control) or were treated for 6 days or 13 days with decidualization stimuli IL1B (10 ng/ml) or dbcAMP (0.1 mM) (both in the presence of SHs. The term *steroid hormones* in this article refers to treatment with a mix of 36 nM estradiol-17 $\beta$  and 1  $\mu$ M medroxyprogesterone acetate (final concentrations). Cell culture medium was changed every 2 days. In decidualization experiments, the medium was collected on Day 6 or Day 12 of treatment and frozen at  $-70^{\circ}\text{C}$  until further analysis. All experiments were repeated a minimum of three times, and each experiment was done in triplicate.

### TAZ Detection by Western Blot

**Cell lysates.** Following each treatment, HuF cells were rinsed twice with PBS and lysed on ice with lysis buffer as previously described [28]. The protein concentration was estimated by Bradford assay (Bio-Rad Laboratories, Inc., Webster, TX). Equal amounts of total protein (35  $\mu$ g) were separated by 4%–20% SDS-PAGE.

**Nuclear and cytosolic fractions.** HuF cells grown in 100-mm plates were subjected to decidualization stimuli for 13 days. The cells were scraped into ice-cold PBS, and nuclear and cytosolic fractions were isolated as previously described [27]. Equal volumes of nuclear and cytosolic fractions were loaded and separated by 4%–20% SDS-PAGE.

The gels with separated samples (cell lysates or nuclear and cytosolic fractions) were transferred onto polyvinylidene difluoride membranes and probed with specific antibodies against TAZ (1:1000; Cell Signaling Technology, Inc.) according to the protocol provided by the manufacturer. The membranes were reprobbed for MYC (c-myc) (1:200; Santa Cruz Biotechnology, Santa Cruz, CA) and beta-actin (1:8000; Sigma) according to the protocols provided by the manufacturers. The immunoreactive bands were detected by enhanced chemiluminescence, and digital images were captured by Quantity One 1-D analysis software on a ChemiDoc XRS System (Bio-Rad Laboratories, Inc.).

### Immunofluorescence Staining

HuF cells grown on glass coverslips were fixed with 4% paraformaldehyde, permeabilized with 0.1% Triton X-100, and then blocked with 5% bovine

serum albumin (BSA) at room temperature (RT). Incubations with primary antibody against TAZ (1:1000; Sigma) were conducted at  $4^{\circ}\text{C}$  overnight, followed by incubation for 1 h with fluorescein isothiocyanate-conjugated secondary antibodies (1:100). Coverslips were mounted with Prolong Antifade containing DAPI and examined using a Zeiss (Welwyn Garden City, UK) LSM 510 laser confocal microscope.

### RT-PCR Analysis and Real-Time PCR

HuF cells (control or after 13 days of decidualization treatments) were lysed in Trizol reagent (Invitrogen), and total RNA was extracted. RNA was subjected to DNase I treatment and reverse transcribed using the iScript cDNA synthesis kit (Bio-Rad Laboratories, Inc.) according to the manufacturer's instructions. Standard PCR (35 cycles) was carried out using primers (50 pmol) specific for human *TAZ* [29], *PRL* (prolactin) [30], *PPARG* [31], *IGFBP1* [32], and *H3F3A* (histone H3.3) [32]. The PCR products were resolved on 2% agarose gels, stained with ethidium bromide, and visualized on a ChemiDoc XRS System (Bio-Rad Laboratories, Inc.). Real-time quantitative PCR (qPCR) was carried out with an ABI PRISM 7700 sequence detection system (Applied Biosystems, Foster City, CA) in a 10- $\mu$ l total reaction volume. Each reaction contained 5  $\mu$ l of 2 $\times$  Fast SYBR Green Master Mix (Applied Biosystems), 1  $\mu$ l of 10 $\times$  diluted first-strand cDNA, and 0.5  $\mu$ M primers (*TAZ* [29] and *H3F3A* [33]) or 1  $\mu$ M primer (*IGFBP1* [34]) and was run for 40 cycles (3 sec at  $95^{\circ}\text{C}$ , followed by 20 sec at  $60^{\circ}\text{C}$ ) after an initial denaturation at  $95^{\circ}\text{C}$  for 20 sec. Melt curves were plotted to establish the absence of confounding nonspecific amplification products, and all primer systems were tested and validated for use in the  $2^{-\Delta\Delta\text{Ct}}$  method. Cycle threshold (Ct) values were determined using Prism SDS software version 2.0 (Applied Biosystems). Relative gene expression levels were calculated using the  $2^{-\Delta\Delta\text{Ct}}$  method with *H3F3A* mRNA serving as a reference gene.

### ChIP Assay

Genomic DNA was cross-linked to nuclear proteins by adding formaldehyde directly to HuF cell culture medium to a final concentration of 1% and incubating at RT for 10 min. Glycine was added to a final concentration of 0.125 M, and plates were incubated for 5 min on a rocking platform to stop cross-linking. The medium was removed, and cells were washed two times with ice-cold PBS, scraped into cold PBS with Protease Inhibitor Cocktail I (EMD Biosciences, La Jolla, CA), and collected by centrifugation. The cell pellets were resuspended in cell lysis buffer (5 mM PIPES [pH 8.0], 85 mM KCl, 0.5% Nonidet P-40, and protease inhibitors), incubated on ice for 10 min, and centrifuged. The pellets were resuspended in nuclear lysis buffer (1% SDS, 10 mM edetic acid [EDTA], 50 mM Tris [pH 8.1], and protease inhibitors) and incubated at RT for 10 min. The lysates were sonicated to result in DNA fragments of 300–600 bp in length. Samples were centrifuged to pellet cell debris, and the chromatin-containing supernatants were saved. Aliquots (15  $\mu$ l) of the chromatin solution were saved as nonimmunoprecipitated input controls. The remaining chromatin solution was incubated with rotation overnight at  $4^{\circ}\text{C}$  with sheared salmon sperm DNA (1 mg/ml) and 100  $\mu$ l of prepared Protein A-coated Dynabeads (100.01D; Invitrogen) in dilution buffer (0.01% SDS, 1.1% Triton X-100, 1.2 mM EDTA, 16.7 mM Tris [pH 8], and 167 mM NaCl) to a total volume of 2 ml. The Dynabeads were prepared 1 day before use by washing 25  $\mu$ l of the bead solution per pull down with 5% BSA in PBS three times and incubating with rotation overnight at  $4^{\circ}\text{C}$  with antibodies against TAZ (NB110-58359; Novus Biologicals), PPARG (sc-7196; Santa Cruz Biotechnology), and nonspecific rabbit IgG (sc-2027; Santa Cruz Biotechnology) diluted to manufacturers' specifications. On the day of use, the Dynabeads were washed with 5% BSA in PBS and resuspended in 105  $\mu$ l of dilution buffer. Beads were washed using a magnetic stand. The Dynabead-chromatin solution was washed twice in low-salt buffer (0.1% SDS, 1% Triton X-100, 2 mM EDTA, 150 mM NaCl, and 20 mM Tris-HCl [pH 8.1]), once in high-salt buffer (0.1% SDS, 1% Triton X-100, 2 mM EDTA, 500 mM NaCl, and 20 mM Tris-HCl [pH 8.1]), four times in LiCl buffer (0.25 mM LiCl, 1% Nonidet-P40, 1% sodium deoxycholate, 1 mM EDTA, and 10 mM Tris-HCl [pH 8.1]), and twice in TE buffer (10 mM Tris-HCl [pH 8.1] and 1 mM EDTA). DNA was eluted from the beads by incubating them in 75  $\mu$ l of elution buffer (1% SDS and 100 mM NaHCO<sub>3</sub>) for 10 min at RT. The supernatants were collected, and the elution was repeated for a total of 150  $\mu$ l per sample. The input samples were brought to 150  $\mu$ l using elution buffer. To de-cross-link the samples, NaCl was added to a final concentration of 200 mM, and the samples were incubated for 16 h at  $65^{\circ}\text{C}$ . The samples were purified using QIAquick PCR Purification Kit (Qiagen, Valencia, CA) according to the manufacturer's protocols. DNA eluted from the spin tubes (chromatin templates) was used for PCR.

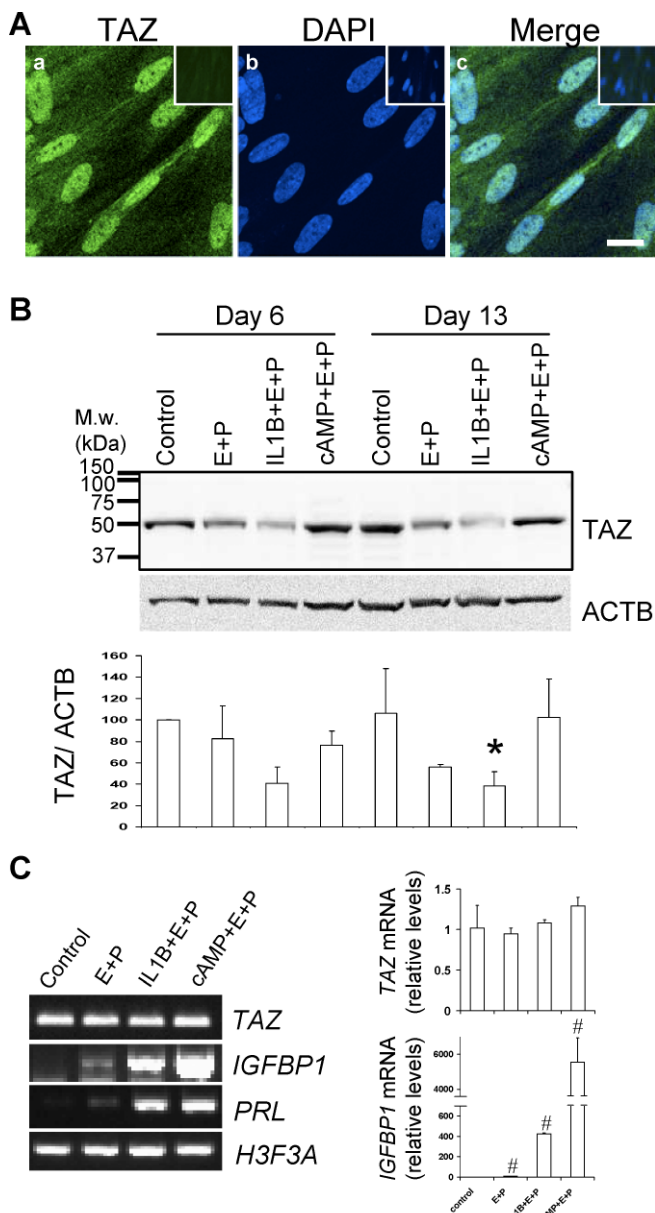


FIG. 1. TAZ detection in HuF cells and its downregulation during in vitro decidualization. **A**) Confocal microscopy of immunofluorescent staining of TAZ in HuF cells (a). Nuclear staining is visualized with DAPI (b). Merge image (c). Bar = 20  $\mu$ m. Nonspecific antibody control staining is in upper corner insets. **B**) Distribution of TAZ in total cell lysates (35  $\mu$ g of protein) of HuF following decidualization for 6 days and 13 days induced by SHs (E+P), IL1B and SHs (IL-1+E+P), cAMP and SHs (cAMP+E+P), and untreated controls (control) as detected by Western blot with TAZ antibody. Membrane was reprobbed with beta-actin (ACTB) antibody (blot below). Densitometric evaluation of TAZ:ACTB ratios is illustrated in graph below blots. The mean value from three experiments for the control at Day 6 was set as 100%. Note the significant difference between control and IL1B- and SH-treated cells on Day 13 (\* $P$   $\leq$  0.05). **C**) TAZ mRNA expression during decidualization. The PCR using primers specific for TAZ, IGFBP1, PRL (prolactin), and H3F3A (histone H3.3) was performed on RNA isolated from HuF cells treated for 13 days as indicated in the figure (left). The qPCR for relative TAZ mRNA levels confirmed no change during decidualization (upper graph), although IGFBP1 mRNA was significantly different between the control and other treatments ( $^{\#}P$   $\leq$  0.05, bottom graph). M.w., molecular weight; E+P, estradiol-17 $\beta$  and medroxyprogesterone acetate.

### PCR of Chromatin Templates

Primers for the following were published previously by Degenhardt et al. [35]: a PPAR response element (PPRE)-containing region located -1197 to -1002 bp relative to the transcription start site (TSS) of the human IGFBP1 gene ([5'-3'] sense: GATCCACCGTTATAGCCTCTG, antisense: CAC-CATCTTTCCTCCCATTC), the control region of IGFBP1 located -8869 to -8377 bp relative to the TSS (sense: CAATTAGGAAGTGCCTCATG, antisense: GACGTTATCATGTTTCAGATTTC), and the TSS of IGFBP1 (-100 to 153 bp) (sense: GAACACTCAGCTCCTAGCGTG, antisense: CTGACATCTCCAGGCGGAG). DNA was used as template with 50 pmol of primers in standard PCR reactions with the following profile: preincubation for 2 min at 95°C, then 50 cycles of 30 sec at 95°C, 30 sec at 60°C, and 30 sec at 72°C, with a final extension incubation of 7 min at 72°C. The PCR products were separated on 2% agarose gels with ethidium bromide and visualized on a ChemiDoc XRS System (Bio-Rad Laboratories, Inc.).

### Statistical Analysis

Statistical analyses were performed using SPSS 15.0 (SPSS Inc., Chicago, IL). Results are expressed as the mean  $\pm$  SD. One-way ANOVA was used to test the null hypothesis of group differences, followed by either a two-tailed  $t$ -test for pairwise comparison or post hoc tests using Tukey and Bonferroni correction for multiple comparisons.

## RESULTS

### TAZ Protein Decreases During In Vitro Decidualization Induced by SHs and IL1B

HuF is a suitable model to study transcription coactivator TAZ because immunocytochemistry confirmed its presence in native cells. Confocal microscopy showed that the majority of the TAZ protein in HuF cells is localized in the nucleus (Fig. 1A). In addition, Western blot analysis with a C-terminal-specific TAZ antibody revealed the presence of TAZ protein as a distinct band of the appropriate size (50 kDa) (Fig. 1B). Detection of TAZ protein in whole-cell lysates revealed that in vitro decidualization of HuF cells is associated with a noticeable decrease in TAZ protein after treatment with SHs alone and an even greater statistically significant decrease after treatment with the embryonic stimulus cytokine IL1B and SHs (38.4%  $\pm$  13.3% when the mean value for TAZ 6-day control was set as 100%) (Fig. 1B). In contrast, widely used artificial decidualization stimulus cAMP (with SHs) did not have any noticeable effect on the level of TAZ protein in cell lysates after 6 days and 13 days of treatment (Fig. 1B). While decidualization treatment with IL1B and SHs resulted in a significant change in TAZ protein level, TAZ mRNA levels did not change as confirmed by qPCR (Fig. 1C). In contrast, the expected increases in mRNA for decidualization markers IGFBP1 and prolactin after decidualization treatments were evident (Fig. 1C).

### TAZ Decline in Nucleus During Decidualization

Because TAZ protein was described as moving between the nucleus and the cytosol, we investigated possible changes in TAZ location during in vitro decidualization for 13 days. In agreement with immunofluorescence staining (Fig. 1A), the majority of TAZ protein in vehicle control (untreated) HuF cells was detected in the nuclear extract (Fig. 2A). Some TAZ protein was also seen in the cytosolic extract (Fig. 2A). Interestingly, the treatment with IL1B for 13 days resulted in a decrease of TAZ protein in nuclear extract, suggesting that the overall TAZ decline noticed in total cell lysates (Fig. 1B) is attributed to the decrease in the nucleus. Nuclear protein MYC was noticeable only in nuclear fractions. In contrast, beta-actin was uniformly distributed in both cytosol and nuclear fractions in all treatments. The densitometric evaluation of cytosol:nu-



clear fractions confirmed the significant disappearance of TAZ protein from the nuclear fraction after IL1B and SH treatment compared with untreated HuF cells (Fig. 2B).

#### *TAZ Is Detected on the PPRE Region Close to the TSS of the IGFBP1 Gene*

Because TAZ was located in PPARG multiprotein complexes in other cells [3], we examined the presence of PPARG in HuF. *PPARG* mRNA was detected by RT-PCR in HuF cells (Fig. 3A), and PPARG protein was seen in nuclear extracts by Western blot (Fig. 3B). Next, we examined the presence of TAZ and PPARG proteins on the genomic region (−1197 to −1002 bp from the TSS) of decidualization marker *IGFBP1* in living HuF cells. The rationale for choosing this particular region was based on a previous study [35] of liver cells in which this genomic *IGFBP1* region, containing a PPRE, was identified as a primary target of PPARs. ChIP experiments revealed that the region with PPRE was occupied by TAZ and PPARG (Fig. 3C). In contrast, the control region without PPRE was occupied by neither TAZ nor PPARG (Fig. 3C).

#### *TAZ In Vivo Localization in the Human and Baboon Endometrium and at the Pregnant Baboon Implantation Site*

In addition to its presence during in vitro decidualization, we investigated TAZ in the human uterine endometrium by immunostaining in paraffin-embedded fixed tissues. During the proliferative phase of the menstrual cycle, there is specific staining for TAZ protein in the human endometrium, specifically in the luminal epithelium and endometrial glands, as well as in the stroma (Fig. 4a), compared with nonspecific isotype-matched IgG control staining (Fig. 4a, inset). During the secretory phase of the human menstrual cycle, there is a decline in specific staining for TAZ, particularly in stromal cells, while the endometrial glands remain positive (Fig. 4b). A similar pattern for TAZ staining was detected in baboon (*P. anubis*) endometrium tissue samples (Fig. 4, c and d). However, qPCR analysis of mRNA in tissue samples from baboons in proliferative and secretory phases of the menstrual cycle revealed no significant differences in *TAZ* mRNA during the menstrual cycle (Supplemental Fig. S1 available at [www.biolreprod.org](http://www.biolreprod.org)). The baboon model also allows us to determine the localization of TAZ during the early days of pregnancy. There is diminished staining for TAZ close to the early pregnancy (Day 30) implantation site in the baboon endometrium (Fig. 4, e and f), comparable to the nonspecific IgG control. This suggests TAZ protein downregulation during early pregnancy and decidualization in vivo.

## DISCUSSION

The physiological significance of TAZ in the human uterus is unknown. It has been proposed that TAZ is a member of the large superfamily of membrane/cytoskeleton-associated transcriptional regulators that globally control the switch between cell proliferation and differentiation [3]. We recently described cytoskeleton-related changes during differentiation of human stromal cells into decidual cells [26, 27]; therefore, we investigated the involvement of TAZ during this process. To our knowledge, data presented herein are the first evidence of TAZ in the uterus and its possible involvement in decidualization.

During in vitro decidualization, there is a decline in overall TAZ protein after SH treatment, and this trend is enhanced

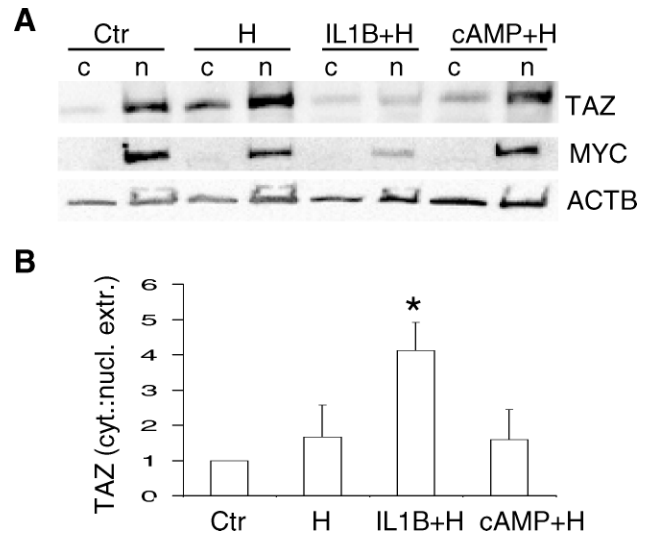


FIG. 2. TAZ decline in nucleus during IL1B-induced decidualization. **A**) Distribution of TAZ in the cytosolic (c) and nuclear (n) fractions of HuF cells treated for 13 days with SHs (H), IL1B and SHs (IL1B+H), cAMP and SHs (cAMP+H), and untreated controls (Ctr) as detected by Western blot with TAZ antibody. Membrane was reprobed with MYC (c-myc) and beta-actin (ACTB) antibodies (blots below). **B**) Quantification of TAZ distribution in cytosol and nuclear extract fractions of HuF cells after 13 days of decidualization treatments expressed as the cytosol:nuclear extract ratio (labeled as cyt.:nucl. extr.) calculated from densitometric evaluation of TAZ bands from three experiments. The mean ratio in control cells (Ctr) from three experiments was set as 1, and other treatments were compared with the control (mean  $\pm$  SD). Note the significant increase ( $*P < 0.05$ ) in the cytosol:nucleus ratio for TAZ in HuF cells treated with IL1B and SHs compared with the control.

significantly in the presence of embryo-mimicking signal IL1B. In contrast, widely used artificial decidualization stimulus cAMP (with SHs) did not have any noticeable effect on TAZ protein, suggesting that TAZ is specifically connected with SH-induced decidualization and is sensitive to the presence of the cytokine. This downregulation of TAZ was not present on the mRNA level, suggesting that its regulation is not on the gene expression level but rather post-translational.

Interestingly, TAZ was recently identified as a downstream effector of the novel Hippo pathway in mammalian cells [8]. The Hippo signaling pathway was originally described in *Drosophila*; however, its components are found in humans, and the pathway is important in the regulation of cell contact inhibition, organ size control, and cancer development [36, 37]. It is believed that the Hippo pathway is coupled with cell differentiation and with organ size such that it is activated when an organ approaches its final size or when cells enter the differentiation phase of development [38]. The decidualization process is the maternal differentiation response in uterine stromal fibroblasts, which functions to inhibit and regulate the invasion of trophoblasts during pregnancy. Thus, the presence of the active Hippo pathway during decidualization is reasonable.

Activation of the Hippo pathway leads to TAZ phosphorylation by its upstream kinase Lats2 [8]. Phosphorylation of TAZ by Lats2 creates a 14-3-3-binding site. Previous findings demonstrated that binding to 14-3-3 promotes the cytoplasmic retention and/or nuclear exclusion of TAZ [2]. As a result, TAZ is sequestered in the cytoplasm and inactivated [8]. This described mode of action is somewhat in agreement with our observation of the diminishing presence of TAZ in the nucleus and its overall decline during decidualization induced by IL1B

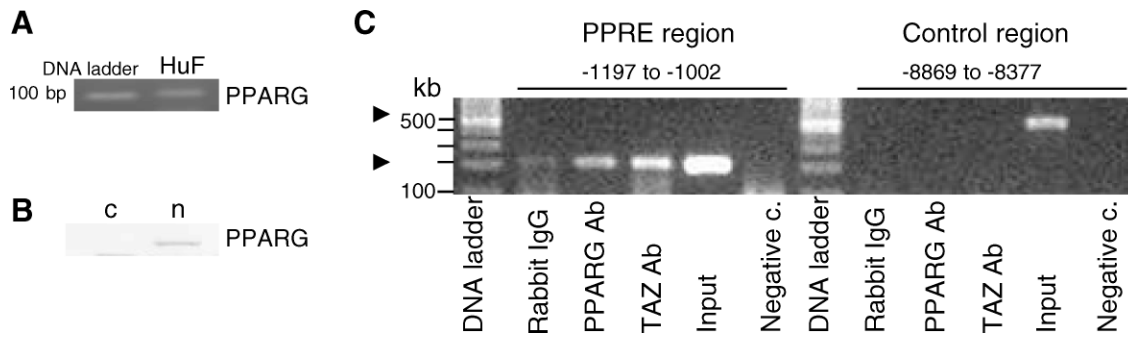


FIG. 3. Association of TAZ and PPARG with the PPRE-containing site of the human *IGFBP1* in vivo. **A**) *PPARG* mRNA in HuF cells detected by RT-PCR in total RNA. **B**) *PPARG* protein detected in the nuclear (n) fraction of HuF cells by Western blot with specific antibody. *PPARG* was not detected in the cytosolic extract (c). **C**) Chromatin was extracted from HuF cells. ChIP experiments were performed with anti-TAZ and anti-*PPARG* antibodies. An association of TAZ and *PPARG* with the PPRE-containing genomic region (-1197 to -1002 bp from the TSS) of the human *IGFBP1* gene was detected. The control region of the *IGFBP1* gene (-8869 to -8377 bp from the TSS), which contains no PPRE, did not show this association. The PCR on the input chromatin template (Input, 1:3100) served as a positive control and that of nonspecific rabbit IgG-precipitated template as a specificity control. Ab, antibody; negative c., negative control.

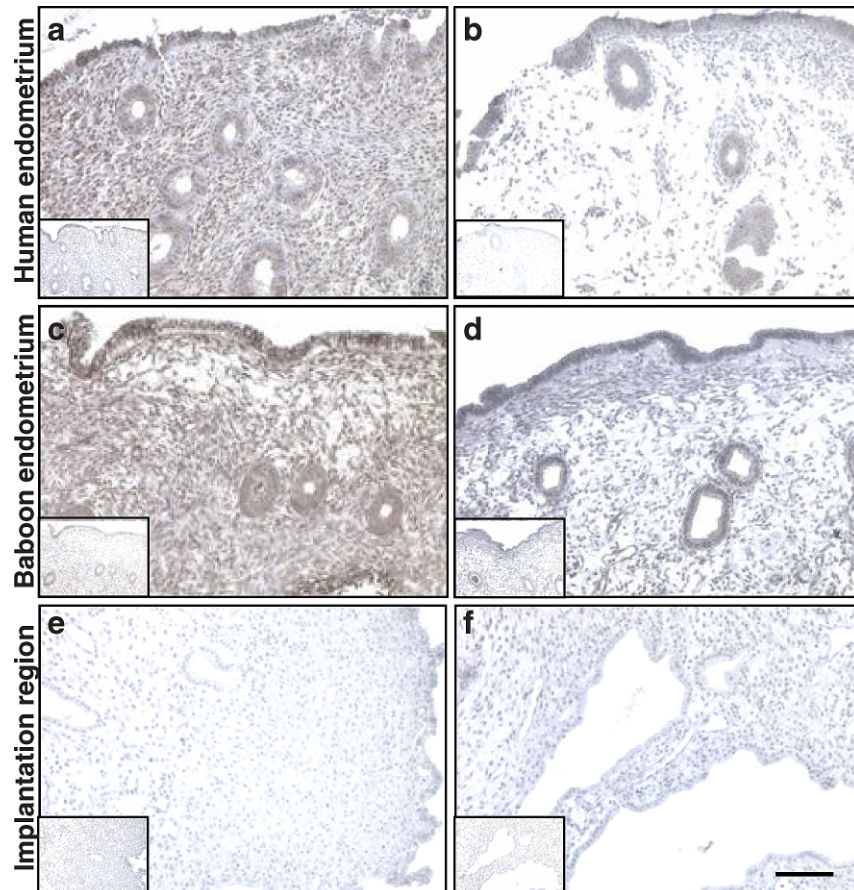
and SHs. *IL1B* is a powerful cytokine having an important role in the regulation of many cellular processes. However, its ability to participate in the regulation of TAZ and presumably to interact with the Hippo pathway has not been previously described to our knowledge.

We reported that *IL1B* induces prostaglandin  $E_2$  ( $PGE_2$ ) synthesis in stromal fibroblasts [19].  $PGE_2$ , a short-lived mediator, is inactivated via an oxidation reaction that generates 15-keto- $PGE_2$ . Interestingly, 15-keto- $PGE_2$  can act as a ligand of *PPARG*, thus activating *PPARG*-mediated transcription [39]. Decidualization-induced downregulation of TAZ is similar to its downregulation (about 50%) reported during

differentiation of mesenchymal stem cells into adipocytes [3, 40]. During that differentiation process, TAZ transcriptionally represses *PPARG*-driven gene expression; its release from the *PPARG*-containing protein multicomplex allows *PPARG*-driven gene expression [3, 40].

*PPARG* has been described as a nuclear regulator of metabolism, differentiation, and cell growth [41]. *Pparg*-null mice are not viable because of defects in placenta formation [9]. In the preimplantation mouse uterus, *PPARG* was identified as a downstream effector of polyunsaturated fatty acid-metabolizing enzymes [10]. Upon ligand binding, *PPARG* releases bound corepressors and recruits coactivators for

FIG. 4. Localization of TAZ in human and baboon endometrium and at the implantation site in the pregnant baboon. Immunohistochemical detection of TAZ in the human endometrium in proliferative (a) and secretory (b) phases of menstrual cycle, baboon endometrium in proliferative (c) and secretory (d) phases of menstrual cycle, and pregnant baboon endometrium (Day 30 of pregnancy) at the implantation site (e and f). Insets show staining with nonspecific control rabbit IgG. Specific TAZ staining is brown. Blue nuclear costaining is with hematoxylin. Note the decline in TAZ staining in the stroma during the secretory phase (b and d) compared with the proliferative phase (a and c). Endometrium at the implantation region shows minimal TAZ staining (e and f). All images are taken at same magnification. Bar = 100  $\mu$ m.





transcriptional activation [42, 43]. The expression of PPAR $\gamma$  in the epithelium and stroma of the pregnant mouse uterus overlapped with the window of implantation [10]. The activation of downstream gene targets of PPAR $\gamma$  was described as important for mouse implantation [10].

We detected *PPARG* mRNA and protein in HuF, confirming the previously observed expression of endogenous PPAR $\gamma$  in human endometrial stromal cells [44]. A number of studies have identified the insulin growth factor (IGF) axis as a target of PPAR $\gamma$  signaling. IGFBP1 is a molecular marker for decidualization. It is believed that its core function in decidual cells is the regulation of IGF-I and IGF-II availability on the maternal-fetal interface [45]. Although we previously described that decidualization treatment of IL1B (with SHs) results in *IGFBP1* gene and protein expression [19], the mechanism of *IGFBP1* gene induction by this stimulus is not known. Recently, the *IGFBP1* gene was also described as a primary PPAR target [35]. Our study points to the possible participation of TAZ and PPAR $\gamma$  in the transcriptional regulation of IGFBP1.

We detected that the PPAR $\gamma$  and TAZ proteins occupy the same PPRE close to the TSS of the human *IGFBP1* gene. A ligand-independent association of PPARs with coactivators has been previously reported and structurally explained [46]. Based on the occupancy of TAZ and PPAR $\gamma$  proteins on this PPRE site, we hypothesize that TAZ is a component of the multiprotein complex regulating transcription of IGFBP1 in HuF cells. The same PPRE site of the IGFBP1 genomic region was associated with all three subtypes of PPARs, their dimer partner retinoid X receptor, and activated RNA polymerase II in the human liver cell line [35]. We hypothesize that PGE<sub>2</sub> release induced by embryonic stimulus (IL1B) serves as a ligand-activating stimulus for PPAR $\gamma$  in the inhibitory multiprotein transcriptional complex that contains the repressor TAZ. As a consequence of ligand binding, TAZ would be released from this complex and transferred to the cytoplasm, where it can be degraded; thus, we detect less of the protein in cells undergoing decidualization by embryonic stimulus. This would allow transcription of the *IGFBP1* gene and decidualization to occur.

TAZ was described as controlling genes important for muscle differentiation [6, 7], lung and respiratory epithelia differentiation [4], cardiac and limb development [5], adipogenesis and osteogenesis [3], and tumorigenesis [47]. For the first time to our knowledge, we report that TAZ is present in the human uterine endometrium. Its decline during the secretory phase of the menstrual cycle, when implantation and decidualization occur, and at the baboon implantation site suggests its possible participation during in vivo decidualization and its involvement in the regulation of early pregnancy.

In summary, we detected a decrease in the protein level of transcriptional regulator TAZ accompanied by its disappearance from the nucleus during in vitro decidualization induced by IL1B (and SHs). We located TAZ and PPAR $\gamma$  proteins in the vicinity of the TSS of the human *IGFBP1* gene, suggesting their possible participation in the regulation of this decidualization marker. Moreover, the in vivo TAZ expression profile is in agreement with findings of in vitro decidualization studies.

## ACKNOWLEDGMENTS

We thank Professor A.T. Fazleabas (director of the Center for Women's Health and Reproduction, University of Illinois at Chicago) for his generous help with tissues, S. Ferguson-Gottschall (Human Female Reproductive Tissue bank at the Center for Women's Health and Reproduction) for obtaining placenta and isolating cells, and P. Mavrogianis (Imaging and Microscopy Core, Center for Women's Health

and Reproduction) for helpful technical assistance with histological samples.

## REFERENCES

- Perissi V, Rosenfeld MG. Controlling nuclear receptors: the circular logic of cofactor cycles. *Nat Rev Mol Cell Biol* 2005; 6:542–554.
- Kanai F, Marignani PA, Sarbassova D, Yagi R, Hall RA, Donowitz M, Hisaminato A, Fujiwara T, Ito Y, Cantley LC, Yaffe MB. TAZ: a novel transcriptional co-activator regulated by interactions with 14-3-3 and PDZ domain proteins. *EMBO J* 2000; 19:6778–6791.
- Hong JH, Hwang ES, McManus MT, Amsterdam A, Tian Y, Kalmukova R, Mueller E, Benjamin T, Spiegelman BM, Sharp PA, Hopkins N, Yaffe MB. TAZ, a transcriptional modulator of mesenchymal stem cell differentiation. *Science* 2005; 309:1074–1078.
- Park KS, Whitsett JA, Di Palma T, Hong JH, Yaffe MB, Zannini M. TAZ interacts with TTF-1 and regulates expression of surfactant protein-C. *J Biol Chem* 2004; 279:17384–17390.
- Murakami M, Nakagawa M, Olson EN, Nakagawa O. A WW domain protein TAZ is a critical coactivator for TBX5, a transcription factor implicated in Holt-Oram syndrome. *Proc Natl Acad Sci U S A* 2005; 102:18034–18039.
- Mahoney WM Jr, Hong JH, Yaffe MB, Farrance IK. The transcriptional co-activator TAZ interacts differentially with transcriptional enhancer factor-1 (TEF-1) family members. *Biochem J* 2005; 388:217–225.
- Kitagawa M. Sveinsson's chorioretinal atrophy-associated missense mutation in mouse *Tead1* affects its interaction with the co-factors YAP and TAZ. *Biochem Biophys Res Commun* 2007; 361:1022–1026.
- Lei QY, Zhang H, Zhao B, Zha ZY, Bai F, Pei XH, Zhao S, Xiong Y, Guan KL. TAZ promotes cell proliferation and epithelial-mesenchymal transition and is inhibited by the Hippo pathway. *Mol Cell Biol* 2008; 28:2426–2436.
- Barak Y, Nelson MC, Ong ES, Jones YZ, Ruiz-Lozano P, Chien KR, Koder A, Evans RM. PPAR gamma is required for placental, cardiac, and adipose tissue development. *Mol Cell* 1999; 4:585–595.
- Li Q, Cheon YP, Kannan A, Shanker S, Bagchi IC, Bagchi MK. A novel pathway involving progesterone receptor, 12/15-lipoxygenase-derived eicosanoids, and peroxisome proliferator-activated receptor gamma regulates implantation in mice. *J Biol Chem* 2004; 279:11570–11581.
- Irving JA, Lala PK. Functional role of cell surface integrins on human trophoblast cell migration: regulation by TGF-beta, IGF-II, and IGFBP-1. *Exp Cell Res* 1995; 217:419–427.
- Hamilton GS, Lysiak JJ, Han VK, Lala PK. Autocrine-paracrine regulation of human trophoblast invasiveness by insulin-like growth factor (IGF)-II and IGF-binding protein (IGFBP)-1. *Exp Cell Res* 1998; 244:147–156.
- Rutanen EM, Pekonen F, Makinen T. Soluble 34K binding protein inhibits the binding of insulin-like growth factor I to its receptors in human secretory phase endometrium: evidence for autocrine/paracrine regulation of growth factor action. *J Clin Endocrinol Metab* 1988; 66:173–180.
- Kearns M, Lala PK. Life history of decidual cells: a review. *Am J Reprod Immunol* 1983; 3:78–82.
- Kliman HJ. Uteroplacental blood flow: the story of decidualization, menstruation, and trophoblast invasion. *Am J Pathol* 2000; 157:1759–1768.
- Karpovich N, Klemmt P, Hwang JH, McVeigh JE, Heath JK, Barlow DH, Mardon HJ. The production of interleukin-11 and decidualization are compromised in endometrial stromal cells derived from patients with infertility. *J Clin Endocrinol Metab* 2005; 90:1607–1612.
- Klemmt PA, Carver JG, Kennedy SH, Koninckx PR, Mardon HJ. Stromal cells from endometriotic lesions and endometrium from women with endometriosis have reduced decidualization capacity. *Fertil Steril* 2006; 85:564–572.
- Foundas SA, Conley YP, Lyons-Weiler JF, Jeyabalan A, Hogge WA, Conrad KP. Altered global gene expression in first trimester placentas of women destined to develop preeclampsia. *Placenta* 2009; 30:15–24.
- Strakova Z, Srisuparp S, Fazleabas AT. Interleukin-1 $\beta$  induces the expression of insulin-like growth factor binding protein-1 during decidualization in the primate. *Endocrinology* 2000; 141:4664–4670.
- Strakova Z, Mavrogianis P, Meng X, Hastings JM, Jackson KS, Cameo P, Brudney A, Knight O, Fazleabas AT. In vivo infusion of interleukin-1 $\beta$  and chorionic gonadotropin induces endometrial changes that mimic early pregnancy events in the baboon. *Endocrinology* 2005; 146:4097–4104.
- Fortman JD, Herring JM, Miller JB, Hess DL, Verhage HG, Fazleabas AT. Chorionic gonadotropin, estradiol, and progesterone levels in baboons (*Papio anubis*) during early pregnancy and spontaneous abortion. *Biol Reprod* 1993; 49:737–742.

22. Markoff E, Zeitler P, Peleg S, Hardwerger S. Characterization of the synthesis and release of prolactin by an enriched fraction of human decidual cells. *J Clin Endocrinol Metab* 1983; 56:962–968.
23. Richards RG, Brar AK, Frank GR, Hartman SM, Jikihara H. Fibroblast cells from term human decidua closely resemble endometrial stromal cells: induction of prolactin and insulin-like growth factor binding protein-1 expression. *Biol Reprod* 1995; 52:609–615.
24. Brar AK, Handwerger S, Kessler CA, Aronow BJ. Gene induction and categorical reprogramming during in vitro human endometrial fibroblast decidualization. *Physiol Genomics* 2001; 7:135–148.
25. Kim JJ, Taylor HS, Akbas GE, Foucher I, Trembleau A, Jaffe RC, Fazleabas AT, Unterman TG. Regulation of insulin-like growth factor binding protein-1 (IGFBP-1) promoter activity by FKRH and HOXA-10 in primate endometrial cells. *Biol Reprod* 2003; 68:24–30.
26. Ihnatovych I, Hu W, Martin JL, Fazleabas AT, de Lanerolle P, Strakova Z. Increased phosphorylation of myosin light chain prevents in vitro decidualization. *Endocrinology* 2007; 148:3176–3184.
27. Ihnatovych I, Livak M, Reed J, de Lanerolle P, Strakova Z. Manipulating actin dynamics impacts human in vitro decidualization. *Biol Reprod* 2009; 81:222–230.
28. Strakova Z, Copland JA, Lolait SG, Soloff MS. ERK-2 mediates oxytocin-stimulated PGE<sub>2</sub> synthesis. *Am J Physiol* 1998; 274:E634–E641.
29. Li B, Shi M, Li J, Zhang H, Chen B, Chen L, Gao W, Giuliani N, Zhao RC. Elevated tumor necrosis factor- $\alpha$  suppresses TAZ expression and impairs osteogenic potential of Flk-1+ mesenchymal stem cells in patients with multiple myeloma. *Stem Cells Dev* 2007; 16:921–930.
30. García-Pacheco JM, Oliver C, Kimatrai M, Blanco FJ, Olivares EG. Human decidual stromal cells express CD34 and STRO-1 and are related to bone marrow stromal precursors. *Mol Hum Reprod* 2001; 12:1151–1157.
31. Liu CH, Hwang SM. Cytokine interactions in mesenchymal stem cells from cord blood. *Cytokine* 2005; 32:270–279.
32. Kim JJ, Jaffe RC, Fazleabas AT. Comparative studies on the in vitro decidualization process in the baboon (*Papio anubis*) and human. *Biol Reprod* 1998; 59:160–168.
33. Hastings JM, Jackson KS, Mavrogianis PA, Fazleabas AT. The estrogen early response gene FOS is altered in a baboon model of endometriosis. *Biol Reprod* 2006; 75:176–182.
34. Buzzio OL, Lu Z, Miller CD, Unterman TG, Kim JJ. FOXO1A differentially regulates genes of decidualization. *Endocrinology* 2006; 147:3870–3876.
35. Degenhardt T, Matilainen M, Herzig K, Dunlop TW, Carlberg C. The insulin-like growth factor-binding protein 1 gene is a primary target of peroxisome proliferator-activated receptors. *J Biol Chem* 2006; 281:39607–39619.
36. Saucedo LJ, Edgar BA. Filling out the Hippo pathway. *Nat Rev Mol Cell Biol* 2007; 8:613–621.
37. Zeng Q, Hong W. The emerging role of the Hippo pathway in cell contact inhibition, organ size control, and cancer development in mammals. *Cancer Cell* 2008; 13:188–192.
38. Yin F, Pan D. Fat flies expanded the Hippo pathway: a matter of size control. *Sci STKE* 2007; (380):pe12.
39. Chou WL, Chuang LM, Chou CC, Wang AH, Lawson JA, FitzGerald GA, Chang ZF. Identification of a novel prostaglandin reductase reveals the involvement of prostaglandin E2 catabolism in regulation of peroxisome proliferator-activated receptor  $\gamma$  activation. *J Biol Chem* 2007; 282:18162–18172.
40. Hong JH, Yaffe MB. TAZ: a beta-catenin-like molecule that regulates mesenchymal stem cell differentiation. *Cell Cycle* 2006; 5:176–179.
41. Rosen ED, Spiegelman BM. PPAR $\gamma$ : a nuclear regulator of metabolism, differentiation, and cell growth. *J Biol Chem* 2001; 276:37731–37734.
42. Desvergne B, Wahli W. Peroxisome proliferator-activated receptors: nuclear control of metabolism. *Endocr Rev* 1999; 20:649–688.
43. Nolte RT, Wisely GB, Westin S, Cobb JE, Lambert MH, Kurokawa R, Rosenfeld MG, Willson TM, Glass CK, Milburn MV. Ligand binding and co-activator assembly of the peroxisome proliferator-activated receptor- $\gamma$ . *Nature* 1998; 395:137–143.
44. Ota K, Ito K, Suzuki T, Saito S, Tamura M, Hayashi S, Okamura K, Sasano H, Yaegashi N. Peroxisome proliferator-activated receptor gamma and growth inhibition by its ligands in uterine endometrial carcinoma. *Clin Cancer Res* 2006; 12:4200–4208.
45. Lee PD, Giudice LC, Conover CA, Powell DR. Insulin-like growth factor binding protein-1: recent findings and new directions. *Proc Soc Exp Biol Med* 1997; 216:319–357.
46. Molnár F, Peräkylä M, Carlberg C. Vitamin D receptor agonists specifically modulate the volume of the ligand-binding pocket. *J Biol Chem* 2006; 281:10516–10526.
47. Chan SW, Lim CJ, Guo K, Ng CP, Lee I, Hunziker W, Zeng Q, Hong W. A role for TAZ in migration, invasion, and tumorigenesis of breast cancer cells. *Cancer Res* 2008; 68:2592–2598.